Hindawi Publishing Corporation
International Journal of Distributed Sensor Networks
Volume 2012, Article ID 972893, 11 pages
doi:10.1155/2012/972893

Research Article

Long-Term Deformation Monitoring of Metro-Tunnel Airshaft Excavation during Construction Stage

L. Ran,[1] T. H. Yi,[2] X. W. Ye,[3] and X. B. Dong[1]

[1] *Hangzhou Metro Group Co. Ltd., Hangzhou 310020, China*
[2] *School of Civil Engineering, Faculty of Infrastructure Engineering, Dalian University of Technology, Dalian 116023, China*
[3] *Department of Civil and Environmental Engineering, The Hong Kong Polytechnic University, Hung Hom, Kowloon, Hong Kong*

Correspondence should be addressed to X. W. Ye, cexwye@polyu.edu.hk

Received 2 August 2012; Accepted 24 August 2012

Academic Editor: Hong-Nan Li

The project of Hangzhou Metro Line 1 is the first metro line of the urban rapid rail transit system in Hangzhou, China, which is one of the largest municipal projects of Hangzhou and is being constructed commencing from March 28, 2007 and expected to be completed by October 1, 2012. This metro line has a total length of 48 km and 34 stations, connecting Hangzhou downtown with the suburban area of the city. Owing to the complex geological condition, harsh construction situation, and immature computational methodology, construction of metro systems is often subjected to considerable sources of uncertainties. To ensure the safety of the adjacent building structures, it is a vital necessity to monitor deep excavations of metro tunnels at their in-construction stage. This paper introduces the instrumentation system for settlement monitoring of a metro-tunnel airshaft of the project of Hangzhou Metro Line 1 during the construction of deep excavation. The long-term settlement data monitored by the measurement markers installed at the surface ground and in the depth direction of the airshaft excavation construction site are analyzed and presented in detail. The obtained results indicate that the settlements at the instrumented locations of the construction site during different construction steps vary steadily in an allowable variation range.

1. Introduction

The subway networks have been recognized as the most efficaciously urban rapid rail transit system and are vital in alleviating the urban traffic congestion problem. In the past decade, a large number of underground railway transportation networks have been opened to operation or are being constructed in the metropolises of China. In the construction of metro systems, deep excavations with large excavation areas, great excavation depths, and complex shapes and geological conditions remain a challenging and high risky task in metropolitan regions, especially in soft soil areas [1, 2]. The deformation and stability of deep excavations are highly affected by the soil characteristics, groundwater variations, and surcharge conditions. In the past several years, a few cases of excessive deformation or instability in braced excavations of metro stations occurred in China. In this regard, field instrumentation and performance evaluation of deep excavations during construction stage are of great importance for quality control and safety assurance [3–5].

Health monitoring of civil and transportation infrastructures at both in-construction and in-service stages has gained increasing concerns and achieved rapid progress with the aid of advanced technologies in sensors and sensing networks, data acquisition and communication, signal processing, and data and information management. Numerous long-term monitoring systems have been designed and implemented for civil and transportation infrastructures worldwide such as high-rise buildings, long-span bridges, and high-speed rails [6–9], while the applications of health monitoring technology to underground structures during construction and operation have not been widely exploited and put into practice [10–12]. In this paper, the instrumentation system for settlement monitoring of a metro-tunnel airshaft of the project of Hangzhou Metro Line 1 during the construction of deep excavation is presented, and the long-term settlement data monitored by the measurement markers installed at the

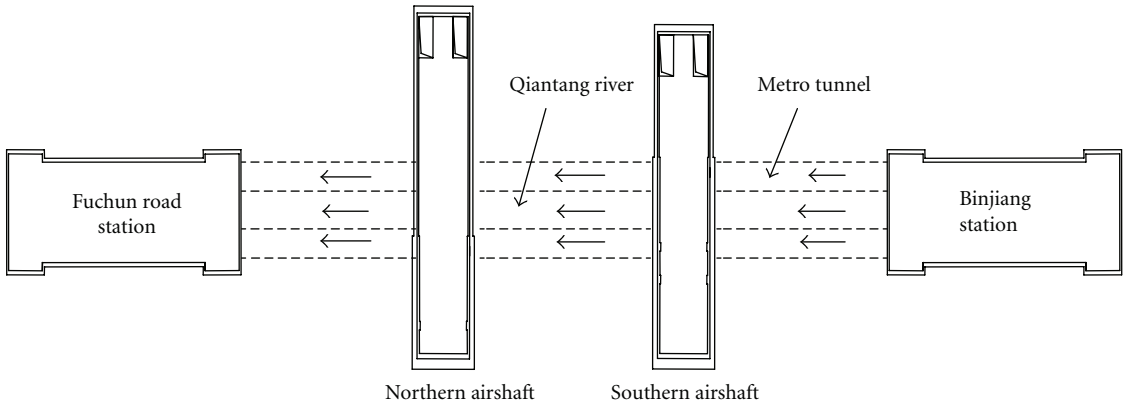

Figure 1: River-crossing metro tunnel and airshafts.

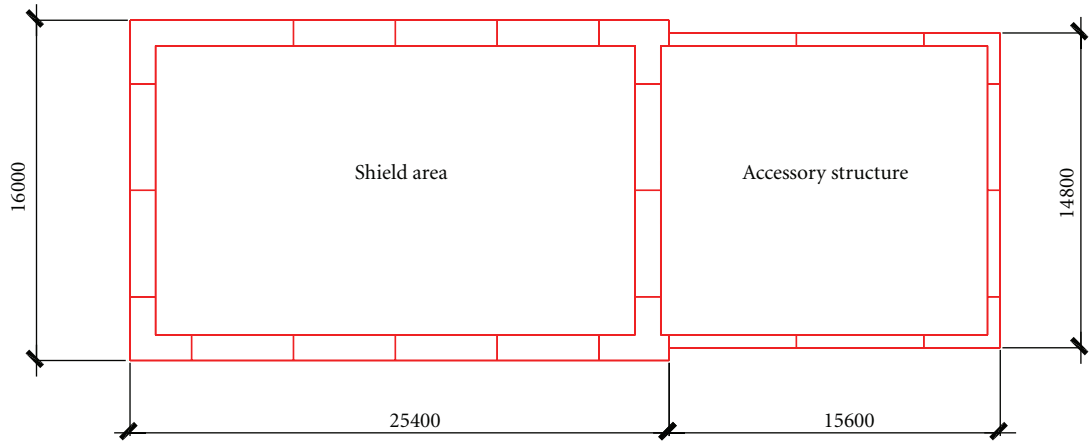

Figure 2: Plan view of southern airshaft excavation.

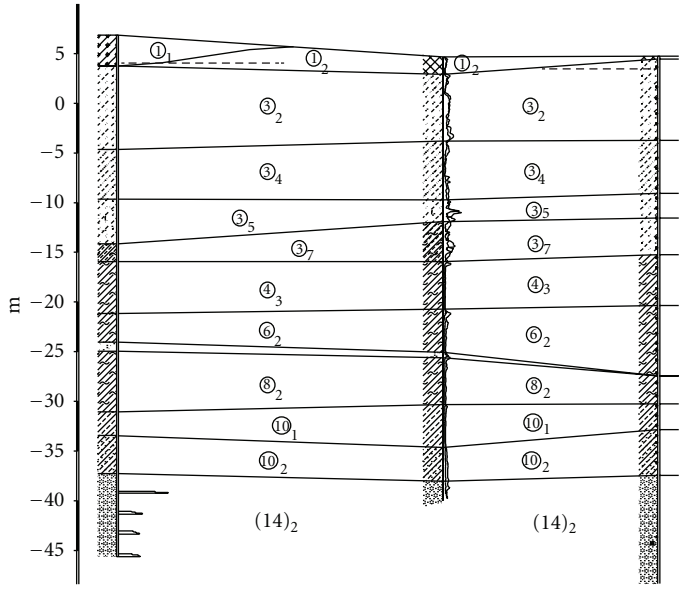

Figure 3: Cross-section of southern airshaft foundation.

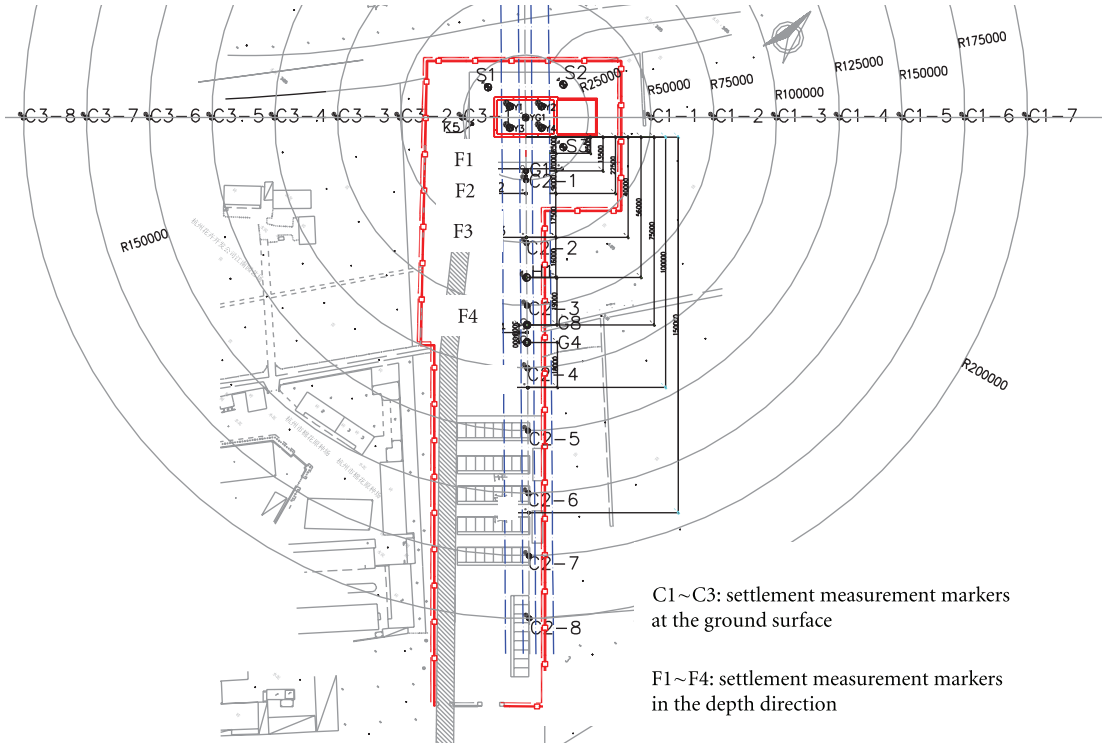

Figure 4: Plan view of deployment locations of settlement measurement markers.

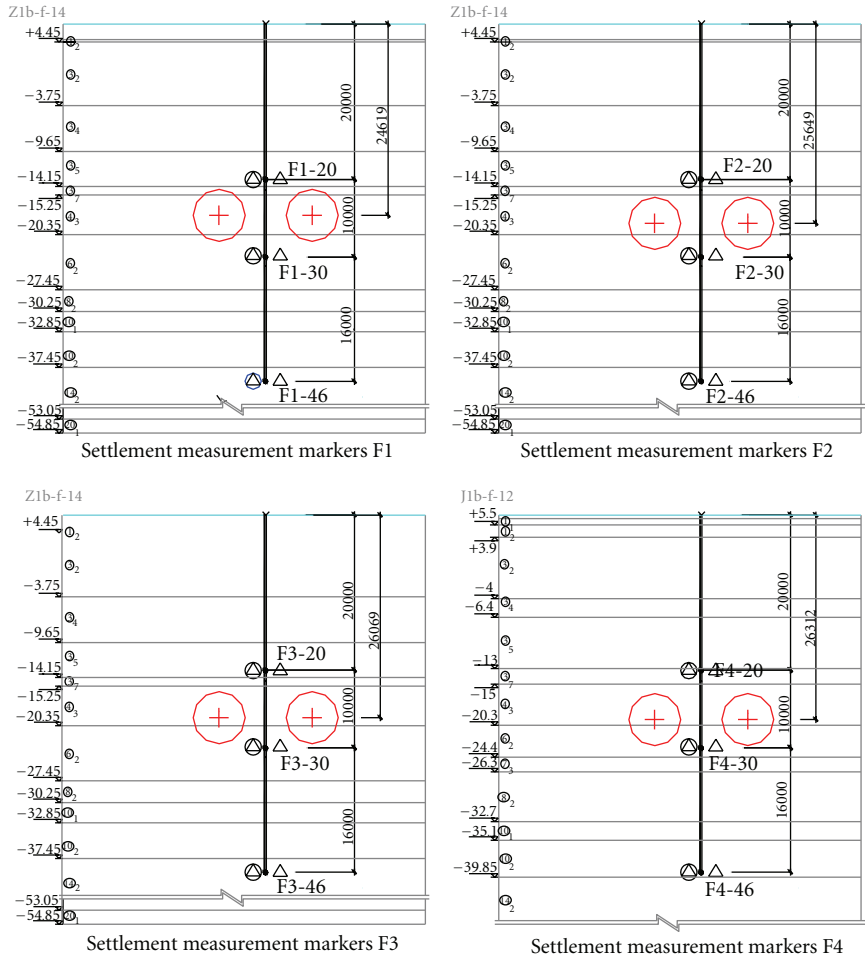

Figure 5: Sectional profile of deployment locations of settlement measurement markers.

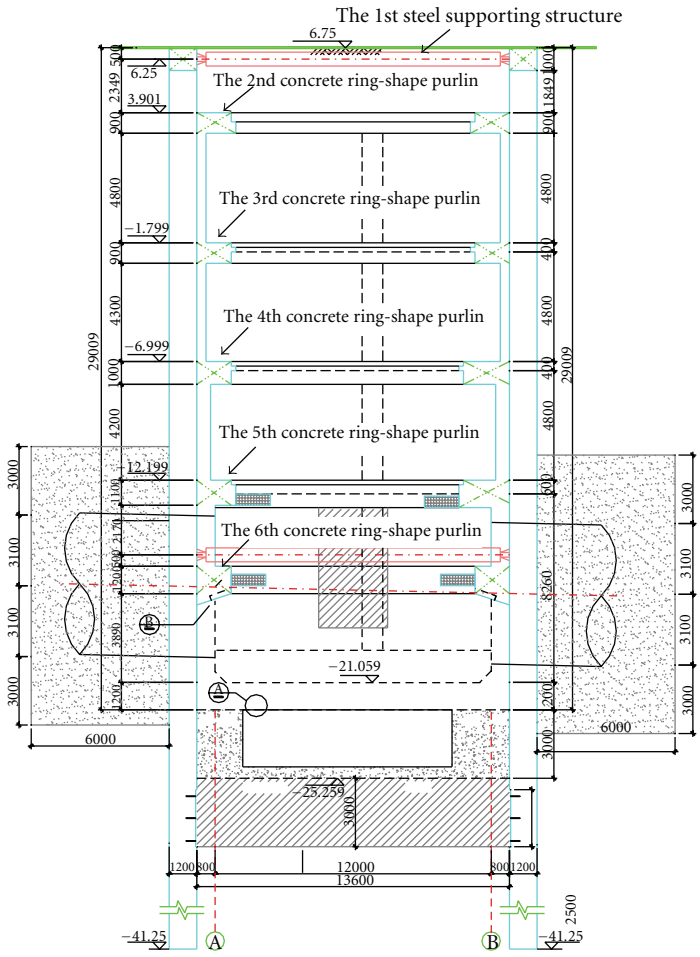

Figure 6: Supporting structures of southern airshaft excavation.

surface ground and in the depth direction of the airshaft excavation construction site are examined.

2. Deep Excavation of Metro-Tunnel Airshaft

As one of the largest municipal projects of Hangzhou, China, the project of Hangzhou Metro Line 1 is the first metro line of the urban rapid rail transit system in Hangzhou which is being constructed commencing from March 28, 2007 and expected to be completed by October 1, 2012. This metro line has a total length of 48 km and 34 stations, connecting Hangzhou downtown with suburban area of the city. It starts from the south at the Xianghu Station in Xiaoshan District, stretches northwards to the Binjiang Station adjacent to the Qiantang River, crosses beneath the Qiantang River to the Fuchun Road Station, passes through Hangzhou downtown, and ends in the Linping Station, with a branch line ending in Xiasha District which diverges from the main line at the Jiubao Station.

The 2nd construction segment of Hangzhou Metro Line 1 covers from the Binjiang Station to the Jiubao Station with a length of 25 km. In this construction section, a two-lane single-bore shield tunnel has been constructed under the Qiantang River to link the Binjiang Station and the Fuchun Road Station, with two airshafts being settled at both sides of the Qiantang River, as shown in Figure 1. In this study, the deformation monitoring of surrounding areas during the deep excavation construction of the southern airshaft will be presented. Figure 2 illustrates the plan view of the southern airshaft excavation with a depth of 29 m.

3. Instrumentation System for Settlement Monitoring

3.1. Engineering Geological and Hydrogeological Conditions. According to the geological characteristics of the construction site of the southern airshaft, the foundation of the southern airshaft is divided into 20 soil layers along the depth of the southern airshaft with the aid of the static cone penetration tests. Table 1 lists the physical and mechanical properties of different soil layers of the southern airshaft foundation. Figure 3 illustrates a typical sectional profile of the southern airshaft foundation in the depth direction. Shallow groundwater at the construction site of the southern airshaft is a layer of porosity diving, mainly existing in the surface soil layers and the soil layers ③$_1$ ~ ③$_8$ of the

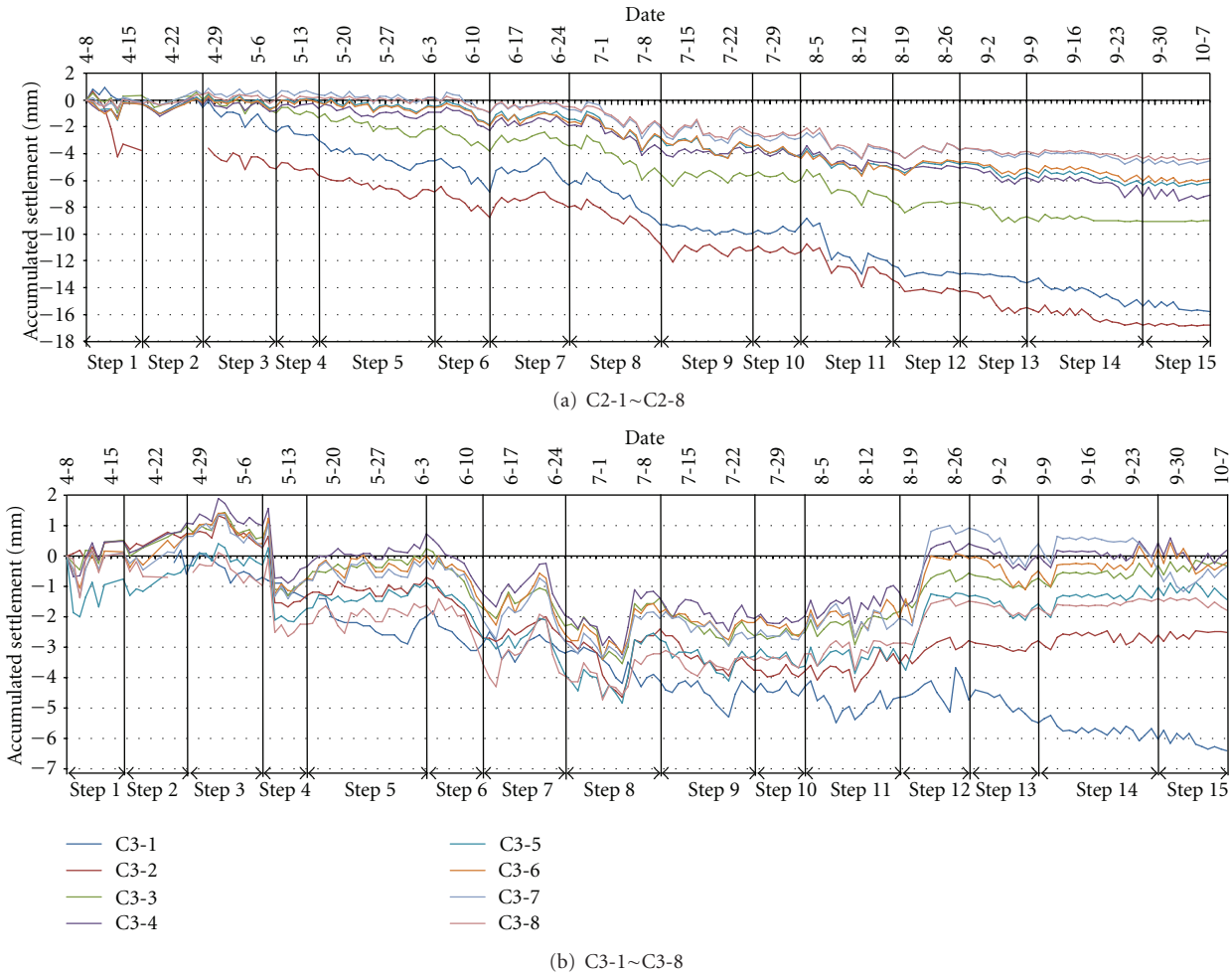

(a) C2-1~C2-8

(b) C3-1~C3-8

Figure 7: Settlement time histories monitored by measurement markers at surface ground.

sandy silt. This layer of groundwater is supplied by the atmospheric precipitation and the surface water runoff, and the groundwater level is largely affected by seasonal changes and the water level of the Qiantang River. Additionally, the construction site of the southern airshaft has two layers of pore confined water, which are distributed in the soil layer ⑥$_3$ and the soil layers $(14)_1$ and $(14)_2$, respectively.

3.2. Instrumentation. To monitor the deformation of the southern airshaft excavation during the construction stage and secure the construction safety, 35 instrumented locations are specified for settlement measurement in parallel with the process of deep excavation construction. Among these monitoring points, 23 settlement measurement markers are located at the ground surface of the construction site, distributing on the circles by taking the central of the southern airshaft excavation as the centre of the circles. The remaining 12 settlement measurement markers are deployed in the depth direction of the southern airshaft excavation, and they are divided into 4 groups in the horizontal direction. The distances between each group of the settlement measurement markers and the underground diaphragm wall of the southern airshaft excavation are 13.5 m, 22.5 m, 40 m, and 78 m, respectively; each group has 3 settlement measurement markers in the depth direction of the southern airshaft excavation with the depths of 20 m, 30 m, and 46 m, respectively. Figures 4 and 5 show the plan view and sectional profile of the deployment locations of the settlement measurement markers distributed at the construction site of the southern airshaft excavation.

4. Analysis of Long-Term Settlement Monitoring Results

The settlements at the instrumented locations are measured during the construction of the southern airshaft excavation, and the settlement monitoring data from April 9, 2008 to October 9, 2008 are extracted and examined in this paper. The deep excavation construction of the southern airshaft excavation can be divided into 15 construction steps, that is, step 1—excavation of the fourth soil layer, step 2—construction of the fourth concrete ring-shape purlin, step 3—construction of the lining wall on the second floor underground, step 4—excavation of the fifth soil

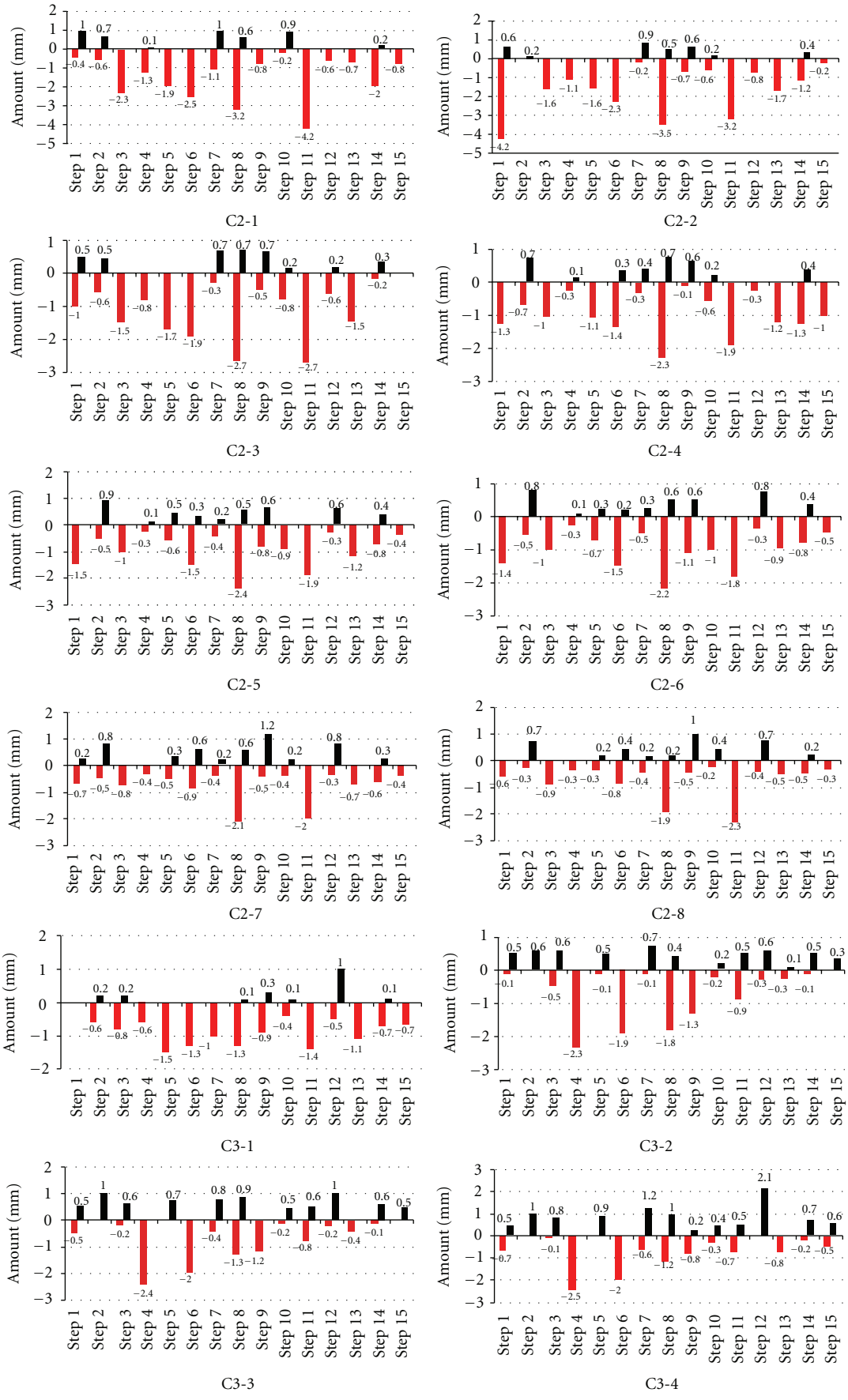

Figure 8: Continued.

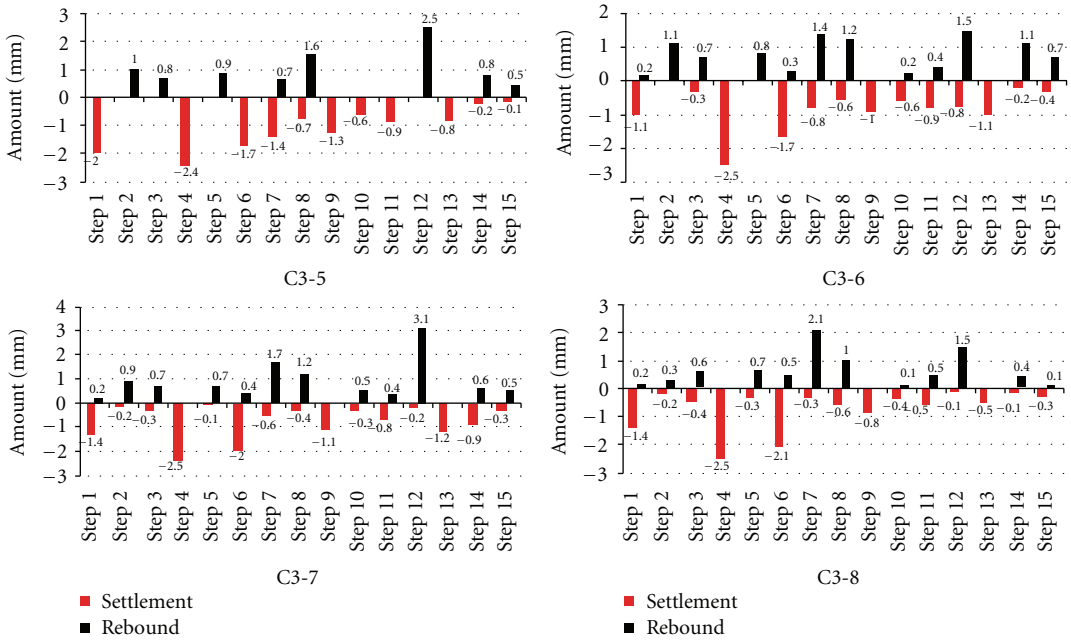

Figure 8: Evaluated settlements and rebounds of instrumented locations at surface ground during different construction steps.

layer, step 5—construction of the fifth concrete ring-shape purlin and supporting structures, step 6—construction of the lining wall on the third floor underground, step 7—concrete curing, step 8—excavation of the sixth soil layer, step 9—construction of the sixth concrete ring-shape purlin, step 10—concrete curing, step 11—excavation of the last soil layer, step 12—base-plate pouring, step 13—base-plate curing, step 14—lining pouring, and step 15—capping operation. Figure 6 illustrates the sectional profile of the supporting structures of the southern airshaft excavation during construction stage.

4.1. Analysis of Monitoring Data at Surface Ground. Figure 7 illustrates the settlement time histories monitored by the measurement markers C2-1∼C2-8 and C3-1∼C3-8 which are instrumented at the surface ground of the construction site of the southern airshaft excavation. It is seen from Figure 7(a) that the accumulated settlements at the locations monitored by the measurement markers C2-1∼C2-8 increase gradually during the whole construction stage of deep excavation of the southern airshaft. The accumulated settlements at the locations monitored by the measurement markers C2-1 and C2-2 are much larger than those at the other locations, and it is because these two settlement monitoring locations are much closer to the southern airshaft excavation than others. A further observation into Figure 7(a) reveals that the settlements during the steps 8 and 11 decline more sharply than those during the other steps, and therefore much attention should be paid to the construction safety control during the excavation of the sixth soil layer (step 8) and the excavation of the last soil layer (step 11).

It can be found from Figure 7(b) that the accumulated settlements at the locations monitored by the measurement markers C3-1∼C3-8 vary nearly in the same trend during the whole construction stage of deep excavation of the southern airshaft. It is also observed from Figure 7(b) that the settlements fluctuate greatly during the step 3 (construction of the lining wall on the second floor underground), the step 4 (excavation of the fifth soil layer), the step 7 (concrete curing), and the step 8 (excavation of the sixth soil layer); while the rebounds dominate the foundation deformation during the step 1 (excavation of the fourth soil layer), the step 2 (construction of the fourth concrete ring-shape purlin), and the step 12 (base-plate pouring). Figure 8 shows the evaluated settlements and rebounds of the instrumented locations at the surface ground of the construction site of the southern airshaft excavation during different construction steps.

4.2. Analysis of Monitoring Data in Depth Direction. Figure 9 shows the settlement time histories monitored by the measurement markers F1∼F4 which are installed in the depth direction of the construction site of the southern airshaft excavation. An insight into Figure 9 reveals that the accumulated settlements monitored by the measurement markers installed at the locations in the depths of 20 m and 30 m increase gradually during the whole construction stage of deep excavation of the southern airshaft, while the accumulated settlements monitored by the measurement markers installed at the locations in the depth of 46 m vary gently during the whole construction stage of deep excavation of the southern airshaft. Figure 10 illustrates the evaluated settlements and rebounds of the instrumented locations in the depth direction of the construction site of the southern airshaft excavation during different construction steps.

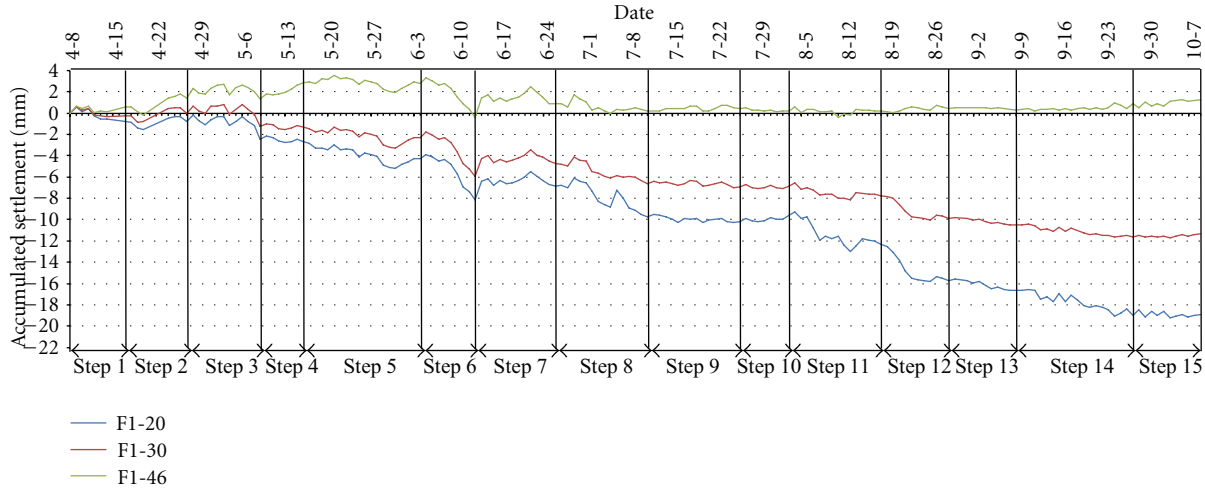

(a) F1-20~F1-46

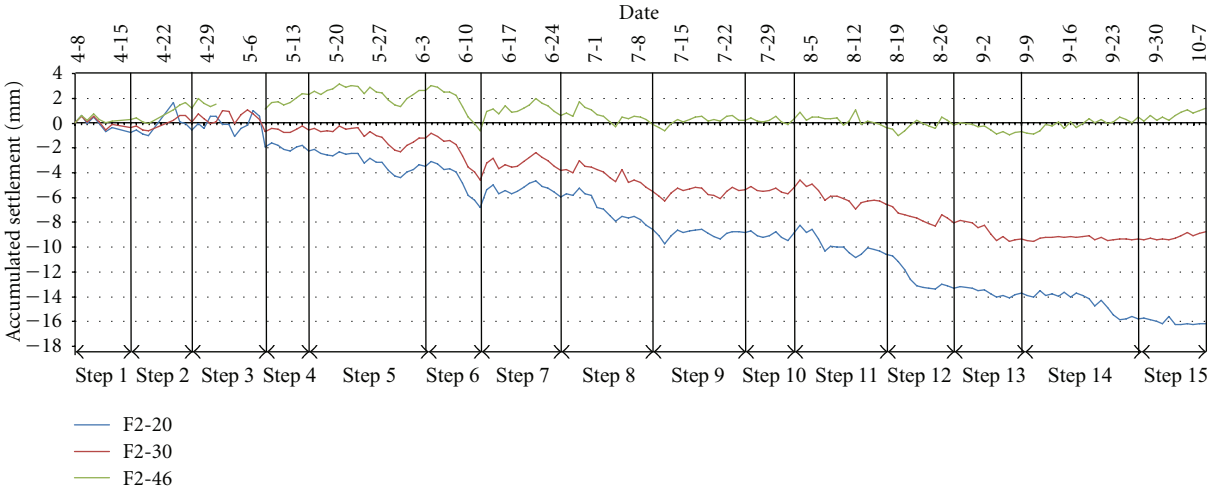

(b) F2-20~F2-46

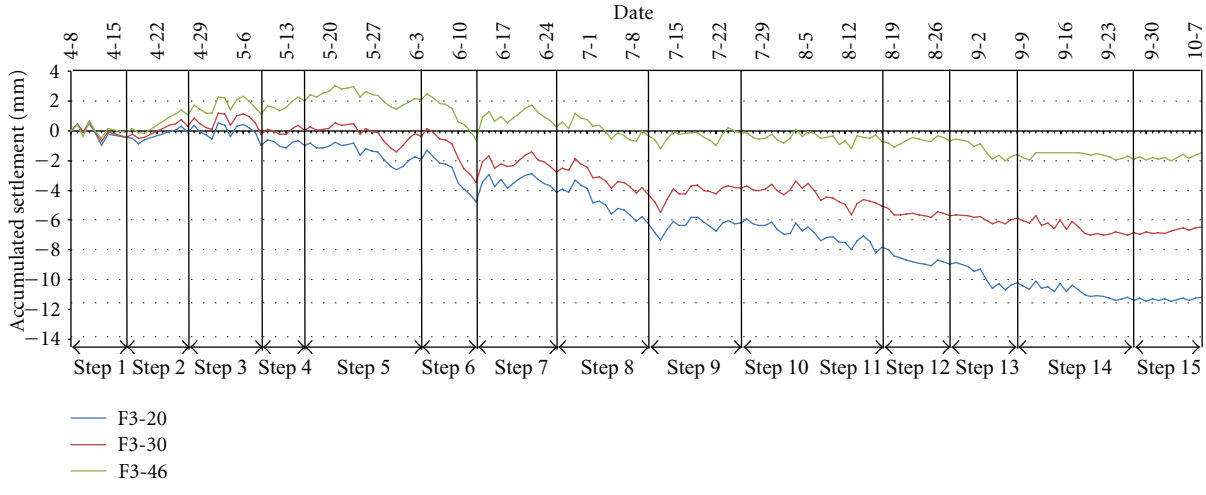

(c) F3-20~F3-46

Figure 9: Continued.

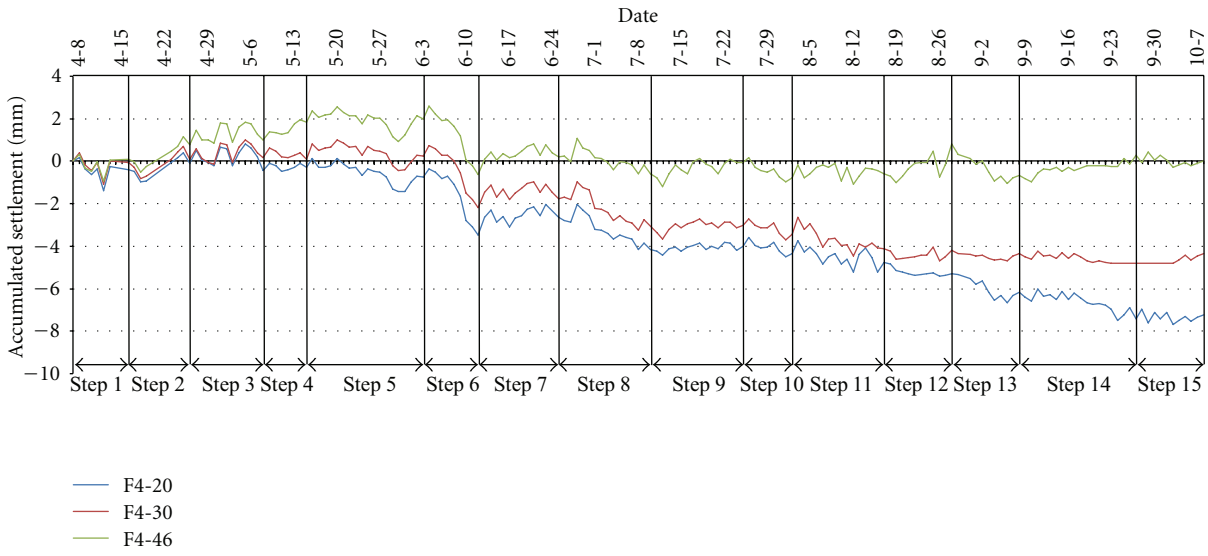

(d) F4-20~F4-46

Figure 9: Settlement time histories monitored by measurement markers in depth direction.

Table 1: Physical and mechanical properties of different soil layers of southern airshaft foundation.

Number	Soil layer	Thickness of soil layer (m)	Physical and mechanical properties					
			Unit weight (kN/m^3)	Specific gravity	Porosity ratio	Saturation (%)	Coefficient of permeability (cm/s)	Modulus of compressibility (MPa)
①$_1$	Miscellaneous fill soil	0.70~3.10	17.5	—	—	—	5.0$E-03$	—
①$_2$	Plain fill soil	0.30~6.00	17.8	—	—	—	8.0$E-04$	6.5
③$_1$	Sandy silt	3.4	17.9	2.70	—	—	4.0$E-04$	7.0
③$_2$	Sandy silt	3.50~9.70	18.4	2.70	0.87	94.2	7.0$E-04$	8.5
③$_4$	Sandy silt	1.00~5.90	18.2	2.70	0.94	95.1	6.5$E-04$	5.5
③$_5$	Silty sand and sandy silt	1.60~7.00	18.2	2.69	0.89	92.5	3.0$E-03$	7.0
③$_6$	Silt	4.20~10.95	18.6	2.69	0.79	89.5	4.0$E-03$	10.0
③$_7$	Sandy silt	0.80~6.20	17.9	2.70	0.95	91.0	2.0$E-04$	5.5
③$_8$	Silt	—	18.3	2.69	—	—	4.5$E-03$	10.5
④$_3$	Silty soft clay	2.60~6.70	17.2	2.73	1.25	96.0	3.0$E-06$	2.6
⑥$_1$	Silty soft clay	1.50~3.70	17.2	2.73	1.16	92.2	2.0$E-06$	2.7
⑥$_2$	Silty soft clay	1.00~8.30	17.4	2.72	1.11	92.3	5.0$E-06$	2.8
⑥$_3$	Silt	0.50~3.85	18.1	2.69	0.82	82.8	3.0$E-03$	8.0
⑧$_2$	Silty soft clay	0.80~8.20	17.3	2.72	1.09	90.4	4.0$E-05$	3.0
⑧$_3$	Silty-fine sand	1.80~8.50	17.7	2.68	0.90	82.8	5.0$E-03$	8.5
⑩$_1$	Silty clay	1.90~4.30	17.4	2.73	1.09	89.7	8.0$E-06$	3.2
⑩$_2$	Silty clay	2.80~4.60	19.6	2.71	0.67	94.1	4.0$E-06$	4.5
(14)$_1$	Medium sand	—	19.9	2.68	—	—	6.0$E-03$	11.0
(14)$_2$	Rounded pebble	—	20.8	2.65	—	—	3.5$E-01$	—

5. Conclusions

Metro-tunnel excavations bring a challenge to the civil engineering community and pose threat to the public safety in metropolitan regions due to the complexity and uncertainty inherent in excavation activities. The stability of deep excavations and adjacent buildings has gained major concerns during metro-tunnel construction. A viable and practical way to ensure the construction safety is by executing real-time monitoring strategy with the aid of advanced

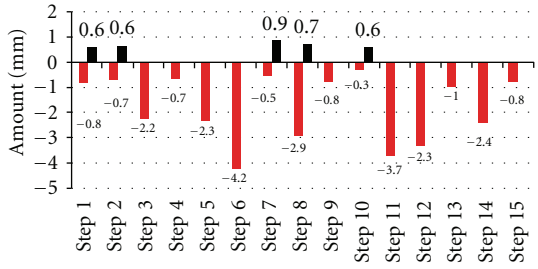

F1-20

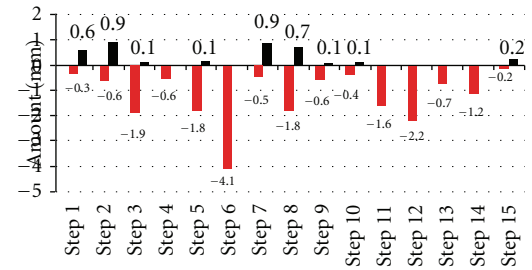

F1-30

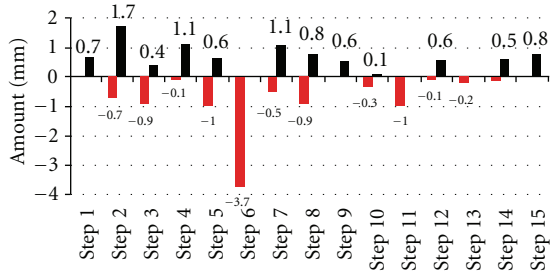

F1-46

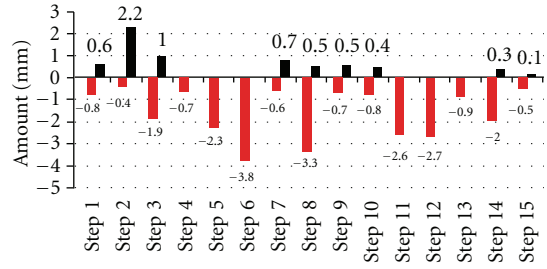

F2-20

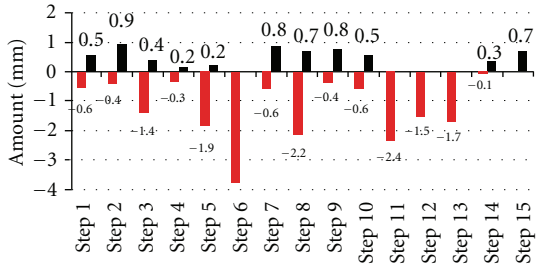

F2-30

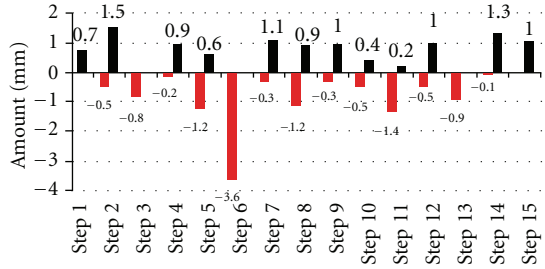

F2-46

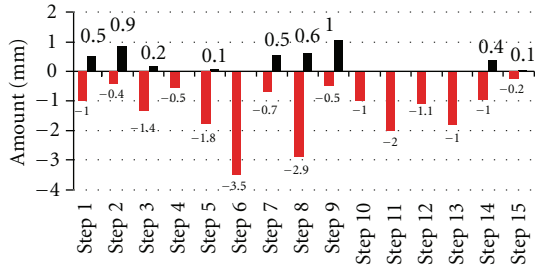

F3-20

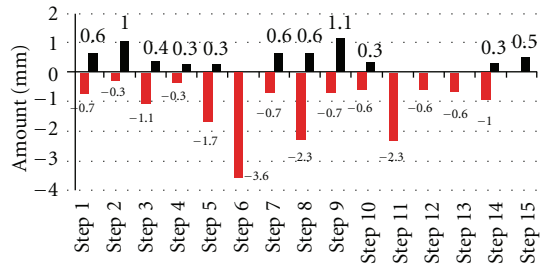

F3-30

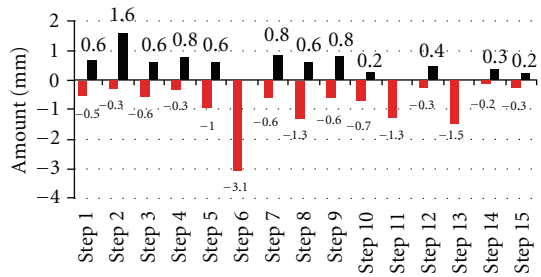

F3-46

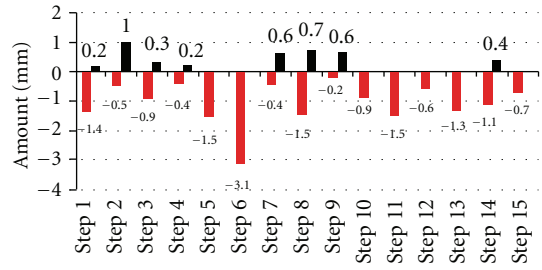

F4-20

Figure 10: Continued.

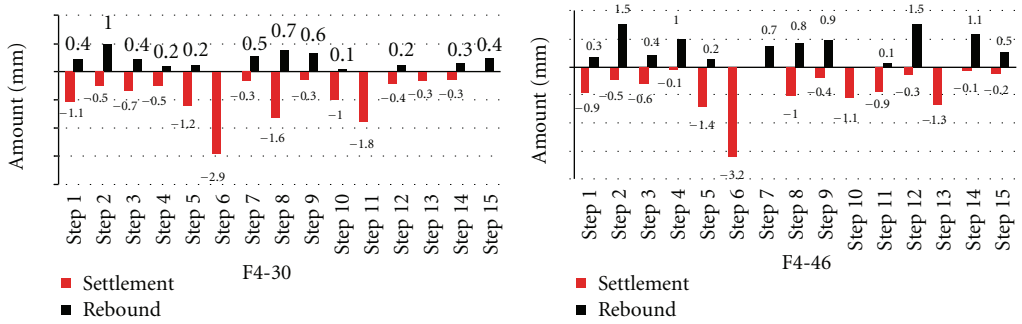

Figure 10: Evaluated settlements and rebounds of instrumented locations in depth direction during different construction steps.

sensing and signal processing technologies. In this paper, an instrumentation system for settlement monitoring of a metro-tunnel airshaft of the project of Hangzhou Metro Line 1 during the construction of deep excavation is presented. After examining the long-term settlement data monitored by the measurement markers installed at the surface ground and in the depth direction of the airshaft excavation construction site, the following specific conclusions are drawn: (i) the accumulated settlements at the locations monitored by the majority of the measurement markers at the ground surface increase gradually during the whole construction stage of deep excavation of the southern airshaft, and the rebounds dominate the foundation deformation during several construction steps; (ii) the accumulated settlements monitored by the measurement markers installed at the locations in the depths of 20 m and 30 m increase gradually, while the accumulated settlements monitored by the measurement markers installed at the locations in the depth of 46 m vary gently during the whole construction stage of deep excavation of the southern airshaft; (iii) the obtained results reveal that the settlements at the instrumented locations of the construction site during different construction steps vary steadily in an allowable variation range.

Acknowledgments

This research work was jointly supported by the Science Fund for Creative Research Groups of the NSFC (Grants no. 51121005), the National Natural Science Foundation of China (Grants no. 51178083 and 51222806), and the Program for New Century Excellent Talents in University (Grant no. NCET-10-0287). The authors also wish to express their thanks to the Hangzhou Metro Group Co. Ltd. for permission to publish this paper.

References

[1] J. Dunnicliff, *Geotechnical Instrumentation for Monitoring Field Performance*, John Wiley & Sons, New York, NY, USA, 1993.

[2] C. Y. Ou, *Deep Excavation-Theory and Practice*, Taylor & Francis, London, UK, 2006.

[3] N. Phienwej and C. H. Gan, "Characteristics of ground movements in deep excavations with concrete diaphragm walls in Bangkok soils and their prediction," *Geotechnical Engineering*, vol. 34, no. 3, pp. 167–175, 2003.

[4] E. H. Y. Leung and C. W. W. Ng, "Wall and ground movements associated with deep excavations supported by cast in situ wall in mixed ground conditions," *Journal of Geotechnical and Geoenvironmental Engineering*, vol. 133, no. 2, pp. 129–143, 2007.

[5] Y. Shao and E. J. Macari, "Information feedback analysis in deep excavations," *International Journal of Geomechanics*, vol. 8, no. 1, pp. 91–103, 2008.

[6] D. Barke and K. W. Chiu, "Structural health monitoring in the railway industry: a review," *Structural Health Monitoring*, vol. 4, no. 1, pp. 81–94, 2005.

[7] J. M. Ko and Y. Q. Ni, "Technology developments in structural health monitoring of large-scale bridges," *Engineering Structures*, vol. 27, no. 12, pp. 1715–1725, 2005.

[8] Y. Q. Ni, Y. Xia, W. Y. Liao, and J. M. Ko, "Technology innovation in developing the structural health monitoring system for Guangzhou New TV Tower," *Structural Control and Health Monitoring*, vol. 16, no. 1, pp. 73–98, 2009.

[9] Y. Q. Ni, X. W. Ye, and J. M. Ko, "Monitoring-based fatigue reliability assessment of steel bridges: analytical model and application," *Journal of Structural Engineering*, vol. 136, no. 12, pp. 1563–1573, 2010.

[10] E. Okundi, P. J. Aylott, and A. M. Hassanein, "Structural health monitoring of underground railways," in *Proceedings of the 1st International Conference on Structural Health Monitoring of Intelligent Infrastructure*, pp. 1039–1046, Tokyo, Japan, 2003.

[11] S. Bhalla, Y. W. Yang, J. Zhao, and C. K. Soh, "Structural health monitoring of underground facilities: technological issues and challenges," *Tunnelling and Underground Space Technology*, vol. 20, no. 5, pp. 487–500, 2005.

[12] P. Wright, "Assessment of London underground tube tunnels—investigation, monitoring and analysis," *Smart Structures and Systems*, vol. 6, no. 3, pp. 239–262, 2010.